CD4 T cell-induced, Bid-dependent apoptosis of cutaneous dendritic cells regulates T cell expansion and immune responses

Sanjay Pradhan[*], **Joseph Genebriera**[*], **Warren L. Denning**[†], **Kumar Felix**[*], **Craig A. Elmets**[*,§], and **Laura Timares**[*,†,‡,§]

[*]Department of Dermatology, University of Alabama at Birmingham, Birmingham AL, 35294, USA.

[†]Department of Cell Biology, University of Alabama at Birmingham, Birmingham AL, 35294, USA.

[‡]Department of Pathology, University of Alabama at Birmingham, Birmingham AL, 35294, USA.

[§]The UAB Skin Diseases Research Center, University of Alabama at Birmingham, Birmingham AL, 35294, USA.

Abstract

The fate of dendritic cells (DCs) after antigen presentation may be DC subset-specific and controlled by many factors. The role of activation-induced apoptosis in regulating DC function is not clear. We investigated the fate of cutaneous DCs (cDCs), specifically Langerhans cells (LCs), and observed that they undergo apoptosis after successful antigen presentation to CD4 T cells. Caspase-specific inhibitors revealed that LC lines utilize a Type II apoptosis pathway in response to CD4 T cells. In support of this, Bid protein was present at high levels and specifically cleaved in the presence of antigen-specific T cells. To test whether Bid was required to regulate LC function *in vivo*, we measured contact sensitization and topical immunization responses in Bid knockout (KO) mice and observed markedly enhanced ear swelling and proliferation responses compared to wild-type (WT) mice. Further, when antigen-pulsed Bid KO migratory cDCs were inoculated into WT recipients, an increase in both the rate and percentage of expanded OT-2 T cells expressing IFNγ was observed. Thus, enhanced antigen presentation function was intrinsic to Bid KO cDCs. Resistance to apoptosis by OT-2 CD4 cells was observed for Bid KO LCs *in vitro*. Therefore Bid is an important regulator of LC viability and antigen presentation function.

Introduction

Langerhans cells (LCs) are a subset of dendritic cells (DCs), which reside in the epidermal layer of skin. They are potent antigen presenting cells that serve as activators of skin-specific immune responses to contact sensitizers, viruses and tumors; More recently they have been implicated in playing a major role for maintaining tolerance to damaged skin proteins (1) (2) (3) (4). As immature DCs, they can capture and process antigen at picomolar concentrations (5), but are weak stimulators of naïve T cell responses. Once a breach in the skin integument is sensed LCs migrate out of the epidermis to dermal lymphatics that lead to draining lymph nodes. As they migrate, LCs lose antigen capture function and gain "mature" DC function, which is completed by their interaction with T cells in the lymph node (6).

Such activated mature DCs have two functions: 1) to activate naïve T cells and 2) to direct T cell differentiation into tissue-specific effector and regulatory cells. Thus LCs determine the magnitude and type of immunologic response made.

Tissue-resident LCs have been shown to possess self-renewing potential, remaining in the epidermis for more than 18 months (7). However, the life span of LCs after they have been activated to migrate to lymph nodes for antigen presentation is not known. Dermal dendritic cells are phenotypically similar to conventional DCs. In the case of conventional dendritic cells, short half-lives have been reported. In spleen it is 1-3 days (8) (9), and in lymph node, antigen pulsed-DC survive for only 24 hours in the presence of antigen-specific T cells (10). Multiple mechanisms may contribute to the brevity of DC life-spans. First, pathogen stimuli sensed through Toll receptors on DCs have been shown to activate an internal "clock" that limits their remaining life span. (11). Such stimuli induces high levels of the proapoptotic "BH3-only domain" protein Bim. Second, once in lymphoid tissue and after antigen presentation, depletion of DC cytokine secretion and /or costimulatory capacity may lead to apoptosis by exhaustion (12). Both of these rely on the intrinsic passive cell death pathway. A third possibility is that an active process of extrinsic death signals derived from successfully activated T cells, hastens the demise of DCs (13). However, in vitro studies indicate that while immature DCs are sensitive to NK, T cell and Fas-mediated apoptosis, mature DCs are resistant (14). Therefore it is not clear if, or at what stage, DCs undergo T-cell mediated apoptosis in vivo, and it is likely that the mechanisms that regulate cell death may be unique for different DC subsets.

Extrinsic apoptotic signals through TNF-family member death receptors utilize two types of caspase signaling cascades (15-17). Type I cells, such as T cells, enable "initiator" caspase 8 to directly activate "executioner" caspase 3. In Type II cells, a specific member of the "Bcl-2 homology domain 3 (BH3)-only " proteins, called Bid (BH3 interacting domain death agonist), has the unique task of linking the extrinsic and intrinsic pathways. Extrinsic signals in Type II cells utilize Bid as the target substrate of caspase 8, generating a truncated active form of Bid that translocates to the mitochondrial membrane and directly activates proapoptotic Bcl-2 family members Bak and Bax. Thus, Bid activates the mitochondrial "amplification loop" leading to apoptosome assembly and caspase 9 activation, caspase 3 activation, and irreversible cell death (18). Although there is much evidence that mitochondrial pro- and anti-apoptotic Bcl-2 family proteins have a profound effect on DC longevity, either in setting the intrinsic clock (11), in modulating Fas-mediated death in vitro (19), or when introduced epigenetically as transgenes (20, 21) (22), it is not clear what type of apoptosis pathway is normally utilized in response to extrinsic signals under physiologic conditions.

In this study we followed the fate of LCs after antigen presentation to CD4 T cells, and found that naïve CD4 T cells were able to induce LC apoptosis in an antigen-specific manner. We then examined what type of apoptotic pathway is utilized in response to extrinsic signals and showed that LC lines are Type II cells, expressing high levels of Bid protein that is activated upon antigen presentation to CD4 T cells. To prove that Bid plays a critical role in regulating LC antigen presentation, we then examined immune responses in topically immunized Bid knockout (KO) mice (23). We observed a marked increase in contact sensitization and topical immunization responses by T cells. Moreover, cutaneous DCs (cDCs) derived from Bid KO mice, could, themselves, impart enhanced T cell responses *in vivo* and demonstrated resistance to CD4 T cell-mediated apoptosis *in vitro*. Thus, our studies indicate that Bid is an important regulator of LC viability and function.

METHODS

Animals and cell lines

Specific pathogen-free A/J mice, C57Bl/6 mice, T cell receptor (TCR) transgenic 3A9 (specific for hen egg lysozyme (HEL) in the context of I-A^k) mice were obtained from Jackson Laboratories (Bar Harbor, Maine; stock #002597) [24]. TCR transgenic CD45.1 OT-2 mice were generously provided by Dr. R. Pat Bucy (University of Alabama at Birmingham). Bid-deficient (referred to here as Bid knockout (KO)) mice on a C57Bl/6 background were generously provided by Dr. Stanley L. Korsmeyer (Harvard Medical Center, Boston MA) [23]. In adoptive transfer experiments where both OT-2 and cutaneous DC were injected, we used albino C57BL/6J-*Tyr^{c-2J}/J* mice from Jackson Laboratories to serve as wild-type (WT) recipients. Mice were bred and maintained under specific pathogen-free conditions at the University of Alabama at Birmingham (Birmingham, AL) and experiments performed with IACUC approved protocols.

The XS106 LC line was established from the epidermis of newborn A/J mice and maintained in vitro, as described previously [25] (obtained as a gift from Dr. Akira Takashima) and demonstrates potent Langerhans cell function in vitro and in vivo[26] [27]. XS106-GFP B1.1 clone was generated by limiting dilution of cells infected with reporter green fluorescent protein (GFP) encoding lentiviral vector obtained as a gift from Dr. Xiaoyun Wu (University of Alabama at Birmingham) ([28] [29]). No functional difference was observed for this cell line, when compared to parental XS106 cells. The 3A9 T cell hybridoma was obtained as a generous gift from Dr. Paul M. Allen (Washington University, School of Medicine, St. Louis, MO) [30].

Medium

For all cell culture and assays, unless noted, we used RPMI 1640 supplemented with heat inactivated fetal bovine serum (10%), L-glutamine (200mM), sodium pyruvate (100mM), Hepes buffer (1M), minimum essential amino acids (100mM), and penicillin/streptomycin (10000 IU/ml) all from Cellgro (Herndon,VA). For XS106 (LC) cell line cultivation we supplemented further with 2-mercapto-ethanol (5mM) (Sigma, St. Louis, Mo.), GM-CSF 0.5 ng/ml (Sigma, St. Louis, MO) and NS47 conditioned supernatant 5%, as described [25].

Cutaneous migratory DC isolation

Mice were anesthetized then antigen applied to tape-stripped ears (10 times) by painting with 25μg OVA or HEL in 10 μl PBS with or without inclusion of 10ng/ml LPS per side or with PBS ± LPS alone, as indicated. After 30 minutes, mice were sacrificed and ear tissue harvested. Ears specimens were split into dorsal and ventral halves, floated dermal side down and cultured for two days in 24-well plates [31]. In some experiments, culture medium additionally contained 100 μg /ml of relevant or irrelevant antigen, as indicated. The cells that migrated from the skin specimens into the culture medium were harvested, passed through a screen to remove large skin debris and examined for cell counts, viability by trypan blue exclusion, and phenotype. Migratory cells routinely contained greater than 50%, I-A and CD11c double positive cells, as determined by flow cytometry [32]. Additionally the I-A positive fraction was 70 – 90% double positive for the Langerhans cell markers, CD205 (DEC-205 Clone NLDC145 from Cedarlane Laboratories Ltd., Ontario, Canada) and Langerin/CD207 (clones 205C1, 929F3) (Abcys Biologie, Paris, France) (data not shown).

Transgenic T cell isolation

Naïve splenic CD4 T cells were purified from either 3A9 or OT-2 transgenic mice using CD4-conjugated Dynabeads in conjunction with the Detach-a-bead kit (Dynal Biotech, Oslo, Norway). The purity of CD4 cells was confirmed by double staining for CD4 and TCR

specific antibodies to the OT-2 TCR expressing Vα5.1 (BD-Biosciences Pharmingen, San Diego CA) or the 3A9 TCR Vβ8.2 (clone F23.2, generously provided by Dr. P. Marrack (33)). Purified T cells were routinely greater than 95% CD4 and TCR positive.

Reagents

Pan caspase inhibitor Z-VAD-FMK, Caspase-8 inhibitor Z-IETD-FMK, Caspase-9 inhibitor Z-LEHD-FMK, caspase inhibitor control Z-FA-FMK (all from R&D Systems, Minneapolis, MN) and Caspase-3 inhibitor Z-DEVD-FMK (Kamiya Biomedical company, Seattle,WA) were used. The following mAb were used: mouse anti-Bid antibody (BD Transduction laboratories, San Diego, CA), monoclonal anti-Beta-Actin clone AC-15 (Sigma, St. Louis, MO), polyclonal rabbit Caspase-3 antibody (Cell Signaling, Beverly, MA), polyclonal Caspase-9 mouse specific (Cell Signaling), polyclonal rabbit anti-Caspase 8 (BD Pharmingen, San Diego,CA), anti-rabbit Ig horseradish peroxidase linked F (ab')2 fragment (Amersham-Biosciences, Piscataway,NJ), anti-mouse Ig Horseradish peroxidase linked whole antibody (Amersham-Biosciences), Annexin V-PE (BD Pharmingen) and FITC anti-mouse I-A/I-E (2G9) (BD Pharmingen). Annexin V binding buffer, 10X (BD Pharmingen). Staurosporine (Sigma), hen egg lysozyme (HEL) (Sigma), 7-Amino-Actynomicin D (7-AAD) (Sigma) and Pierce BCA Protein Assay (Pierce, Rockford, IL) were used.

Western Blots

Cell protein lysates were obtained from pellets of 10^7 cells, washed twice with phosphate buffered saline (PBS) (Cellgro) and dissolved in 100 μl lysis buffer containing Tris-HCL (50mM, ph 7.4) NaCl (150 mM), 10% Np-40, 1 mM EDTA, 0.5% PMSF (1 mM), 0.5% Na_3VO_4 (1mM), 0.5% NaF, 0.1% Leupeptin, 0.1% Apoprotinin. Protein concentrations were determined using the Pierce BCA Protein Assay (Pierce, Rockford,IL) and the BioRad Model 550 microplate reader and the Microplate manager 4.01 software with an absorbance of 565nm.

Proteins were subject to electrophoreses in Biorad ready gel 12% Tris-HCL (BioRad, Hercules,CA) and transferred to BioRad nitrocellulose membranes (BioRad). RNP800 molecular weight marker was used (Amersham-Biosciences) to determine protein sizes. Membranes were blocked with 2% ECL Advance blocking agent (Amersham-Biosciences) and hybridization was performed with the indicated primary antibodies. Murine monoclonal antibody to Bid was used at 1:1000 (Clone 14F2A8, Zymed Laboratories Inc., San Fransisco CA), and murine monoclonal antibody to β-actin (clone AC-15, Sigma) was used at 1: 2×10^6. ECL Advance western blotting detection kit from Amersham Biosciences was used. After incubation with appropriate secondary antibodies, bands were visualized using the ECL advance western blotting detection kit (Amersham-Biosciences). Densitometry analyses were performed on a Macintosh computer using the public domain NIH Image program (developed at the U.S. National Institutes of Health and available on the Internet at http://rsb.info.nih.gov/nih-image/).

Apoptosis assays

Cutaneous DCs were isolated from the supernatant of 2-day mouse ear skin organ cultures. DCs were further cultured overnight in 100μg/ml of antigen (hen egg lysosyme (HEL) or chicken ovalbumin (OVA) (Sigma) protein and / or antigen specific T cells (3A9 T hybridoma or purified CD4 transgenic cells (HEL-IAk specific) or OT-2 CD4 T cells (OVA-I-A^b specific) at a ratio of 1:4 LC:TC. After overnight culture (18 – 24 hours) cells were spun down at 300 g for 10 minutes and incubated 30 minutes on ice with 100 μl of Annexin Binding buffer (1X) (BD Pharmingen) with 3 μl of Annexin V-PE (BD Pharmingen) and FITC–anti-I-Ak (2G9) (BD Pharmingen) and/or APC-CD11c (HL3) (BD Pharmingen) per sample. In some experiments biotinylated-Langerin/CD207 (205C1) (Abcys Biologie, Paris,

France) and PE-CD205/DEC205 (NLDC-145) (Cedarlane Laboratories, Ontario Canada) were used. All isotype controls were purchased from BD Pharmingen. After washing the samples with Annexin Binding buffer, pelleted cells were resuspended in 400µl of Annexin Binding buffer containing 2.5 µg/ml of 7-AAD (Sigma). Multi-parameter flow cytometric analysis of PE–Annexin V and 7-AAD staining was performed gated cells as indicated.

XS-GFP (clone B1.1) cells were pulsed with 100µg/ml HEL (Sigma) overnight then mixed with either 3A9 T cells or unlabeled XS106 as a negative control. One hour prior to mixing cells they were pre-incubated with the following caspase inhibitors: Z-VAD-FMK 100µM, Z-DEVD-FMK 200µM, Z-LEHD-FMK 150µM and Ac-IETD-CHO 200µM and then continuously cultured in the presence of these inhibitors. In some experiments, the positive control for apoptosis were cells treated with Staurosporine (Sigma) (500 nM) overnight. Apoptosis levels were assessed after 16 -20 hours, XS-GFP were gated by green fluorescence and analyzed for apoptosis by PE-Annexin V and 7AAD staining (as described previously). Bar graphs of % Apoptosis values include the loss of GFP positive cells that occurs in late stages of apoptosis and therefore unavailable for cytometric analysis, and adjusted for non-specific toxicity of peptides, as determined in control cultures and is calculated as follows: In this example LCs are GFP positive, in other experiments LC may be stained with other markers, such as Langerin instead. % Specific Cell Death = [% Specific LC Loss] + [Specific Apoptotic Fraction of remaining % LC] where % Specific Loss =[Control (Ctrl) % GFP cells – Experimental (Exp) % GFP cells] and Specific Apoptotoic Fraction of remaining % LC = [Exp fraction of apoptotic cells (% Annexin V and/or 7AAD positive/100) x % Exp GFP cells) – (Ctrl fraction of apoptotic cells x % Ctrl GFP cells)].

Whole mount immunofluorescence

The density of epidermal LCs was ascertained from whole mount epidermal sheets stained for MHC class II molecules. Ear specimens were split and cartilage removed from the dermal side of the dorsal half. Ear epidermis was lifted from the dermis after floating the specimens' dermal side down in 0.5 M ammonium thiocyanate (Sigma, St. Louis, MO) in PBS for 20 minutes. Epidermal sheets were fixed with cold acetone and washed in PBS. Blocking antibody solution (clone 2.4G2 hybridoma from ATCC, 10µg/sample) was added and incubated 1h at 4°C. LCs were labeled with FITC-anti Ia antibody (clone 2G9, BD-Pharmingen, 1 µg/sample) and incubated at 4°C overnight. Excess antibody was washed from sheets by three 30 min incubation with cold PBS then mounted in 0.2% n-propyl gallate-glycerol. Images at 20x magnification were captured (MetaMorph Imaging System, Universal Imaging Corp. Downington, PA) and the number of positive cells counted by a 3rd experimenter blinded to sample identity.

Contact sensitization assays—Mice were sensitized then challenged with the hapten 2-4-dinitrofluorobenzene (DNFB) to elicit a contact hypersensitivity response as per Xu et. al. (34). For the induction phase, hapten painting treatment occurred on Day 0 and Day 1 as follows: Four age-matched mice per group of WT or Bid KO were sensitized with either vehicle only (4:1 Acetone & Olive oil) as a negative control or 0.5% DNFB (Sigma-Aldrich St. Louis MO) by application of 25 µl on the shaved abdomen and 5 µl on each footpad per mouse. On Day 5 post sensitization, a base line measurement of ear thickness was taken using an engineer's micrometer (Mitutoyo Precision, USA, Inc., Elk Grove Village, IL). Elicitation was induced by painting the ears of both vehicle control and sensitized mice with 10 µl of 0.2% DNFB per dorsal and ventral sides of each ear (referred to as Day 0 with respect to day of challenge). Ear thickness measurements of each mouse was taken each day thereafter, as indicated. The averages of ear thickness over baseline measurements for each

group (n=5) is shown and expressed in μm. The magnitude of the swelling response is given as the mean and SEM of each group.

Adoptive transfer experiments—Purified OT-2 T cells (~5×10^6/ml) were labeled with 1 μM CellTracker™ Green CMFDA (synonymous with carboxyfluorescein diacetate succinimidyl ester, CFSE) (Molecular Probes Inc., Eugene, OR) for 8 minutes at room temperature, then neutralized with 20% FBS-PBS and washed 3 times. Cells were adjusted in PBS to deliver 1 - 2×10^6 cells by injecting $100 - 200$ μl intravenously (i.v.) into the tail vein of WT or Bid KO mice. In some experiments, CFSE-OT-2 T cell injected WT mice also received 5×10^4 cutaneous migratory DC from WT or Bid KO skin cultures (as described above) in 20 μl of PBS into the right footpad. After 3 days, mice were sacrificed for harvesting spleen and draining popliteal lymph nodes, which were weighed and prepared for single cell suspension. Cell suspensions were stained with transgenic T cell receptor-specific antibodies and in some cases with the activation marker CD69 (as indicated) and the fluorescence intensity of CFSE was detected by flow cytometric analysis using a BD FACSCalibur system (BD Biosciences, San Jose, CA).

Intracellular cytokine assays—WT mice were injected with 2×10^6 purified allotypically marked CD45.1 positive OT-2 T cells. Groups of mice (n=3) were immunized either topically with OVA (as described above) as a positive control or cDC-immunized by injection of 2×10^5 migratory DC, from OVA painted WT or Bid KO ear skin cultures, into the right footpad. Mice were sacrificed after 4 days and single cell suspensions from draining lymph nodes and spleen from each of the mice were prepared individually by collagenase D digestion. Lymph node cells were prepared immediately for cytokine secretion assay. Spleen cells were subjected to a re-stimulation culture period of 3 days in the presence or absence of 100μg/ml OVA prior to intracellular cytokine assay. To activate cytokine synthesis, lymph node and spleen cells were cultured for 6 hours with Golgi-Stop™ (BD-Biosciences), 50 ng/ml PMA (Sigma) and 500ng/ml calcium ionophore A23187 (Sigma) following BD Cytofix/Cytoperm™ kit instructions. Following treatment, cells were treated with Fc receptor block, and stained with FITC-anti-CD3, biotinylated-anti-CD45.1 and PerCP-conjugated-streptavidin. After fixation/permeabilization, intracellular cytokines were stained with PE-anti IL4 and Alexa 647-anti-IFNγ antibodies (all from BD-Pharmingen). Flow cytometric analysis was performed on a FacsCalibur using CellQuest Pro™ software.

Statistical analysis—One-tailed Student's t-test was applied, and the p-values are indicated in the text and figure legends.

Results

The XS106 LC line and primary LCs are susceptible to antigen-specific T-cell mediated apoptosis

To test whether LCs are down regulated by apoptosis in a T-cell specific manner, we examined the susceptibility to apoptosis of both migratory murine cDCs and the epidermal-derived LC line, XS106, upon antigen presentation to specific 3A9 T cell hybridoma in 18 – 24 hour cultures (Figure 1 A, B). To more easily track XS106 cells in mixed cell assays we developed a series of stable GFP transfectants of XS106. Using a XS-GFP clone we tested the role of specific or non-specific T cells in mediating apoptosis. Importantly, we extended these studies to test if normal, naïve splenic T cells also induced apoptosis in LC lines (Figure 1C).

The results show that both LCs (analysis gated on I-A^{High} expressing cells rerpresenting LCs derived from skin explant cultures) and the XS-GFP line, are highly susceptible to apoptosis mediated by antigen-specific T cell hybridomas in a T cell-specific and antigen-specific manner (Figure 1 A, B). Moreover, naïve CD4 transgenic T cells are also potent inducers of XS106 cell apoptosis (Figure 1c). The XS-GFP line has potent antigen presenting function, since successful T cell activation occurs in these cultures, as shown by CD69 expression and TCR down regulation (Figure 1D), as well as antigen-specific IL-2 secretion (Figure 1E). In time course studies to determine the kinetics of LC death, we have observed little apoptosis within 8 hours (data not shown). This late timing ensures that LC activation, effective antigen presentation and activation of antigen-specific T cells are completed prior to LC apoptosis.

Caspase inhibitors block T cell-mediated LC apoptosis

To investigate which caspase pathway (Type I or Type II) is activated in LCs during T cell interaction, we utilized selective caspase inhibitor peptides and tested them on the XS-GFP line. We reasoned that the Caspase 9 inhibitor peptide (LEHD) would only have blocking activity if LCs were Type II cells while all other caspase inhibitors should block regardless. After peptide preincubation of XS-GFP, 3A9 T hybridoma cells were added at a 1:4 ratio then incubated further overnight. Flow cytometric analysis on gated GFP positive cells revealed that during interaction with T cells, dendritic cell apoptosis was markedly blocked with pan caspase inhibitors, as well as the specific caspase inhibitor for caspase 3, and partially blocked with inhibitors with specificity for either caspase 8 or 9 (Figure 2). Figure 3A shows a significant decrease in Annexin V positive cells for all caspase inhibitors tested; however, peptide-induced toxicity did occur in some samples, as indicated by an increase in single-positive 7AAD staining. This peptide-induced toxicity pattern of staining was also present in parallel control cultures (without T cells, data not shown). Figure 2B shows the compilation of 4 independent experiments (mean ± sem) adjusting for background toxicity and including the quantification of LC loss that occurs, in addition to detecting apoptosis (as shown in Figure 2A) of the remaining cells per sample (see Materials and Methods for details). The finding that inhibitors for caspase 9 have an impact on T cell-mediated LC apoptosis suggests that LCs use, at least partially, the Type II caspase activation cascade.

The 'BH3-only' molecule Bid, essential in Type II Death receptor signaling, is expressed at high levels in LCs and is activated in the presence of T cells

In Type II cells, caspase 8 does not directly cleave procaspase 3, rather it cleaves the protein Bid, generating the active form called truncated Bid (tBid). tBid translocates to the mitochondria where it activates Bak and Bax pro-apoptotic BCL-2 family proteins, culminating in the activation of caspase 9 and resulting in apoptosis (18). To verify the type II character of the apoptosis pathway in LCs, we looked for the presence of Bid in protein lysates of our LC lines, as detected with a full-length Bid-specific mAb in Western blots (Figure 3). As expected, Bid was detected in lysates from WT spleen but not from the splenocytes of Bid KO mice. Bid protein was not detected in T cells, such as 3A9 T hybridoma cells or naïve CD4 T cells, known to be Type I cells. However, high levels of Bid protein were observed in our LC line. LC Bid protein could be activated (cleaved) by staurosporine treatment (Figure 3a) and, significantly, after antigen presentation to T cells (Figure 3 b, c), reducing the Bid-specific signal by 99% and 43% in the presence of 3A9 T hybridoma and naïve CD4 T cells, respectively (Figure 4d). (Activation is detected by disappearance of full-length Bid due to activation-induced cleavage of the Bid-specific mAb epitope.) The specific expression of Bid in LCs, and the demonstration that Bid is cleaved in response to apoptotic stimuli provides further evidence that LCs use the Type II caspase cascade.

Enhanced contact sensitivity responses in Bid KO mice

A stringent proof for the role of Bid in regulating LC apoptosis was investigated using Bid KO mice. We examined whether a loss-of-function mutation in the Bid gene could affect the immune response to topical antigens using a number of model systems.

C57Bl/6 (B6) Bid knockout (KO) mice and wild-type (WT) control B6 mice were sensitized on the abdomen and challenged 5 days later on the ears with the hapten dinitrofluorobenzene (DNFB). Ear swelling responses were accelerated in Bid KO mice and enhanced more than 2-fold over WT mouse responses (Figure 4A). After 5 days post challenge cellular infiltrates could still be seen in epidermal layers of Bid KO, while cellular infiltrates were mainly seen only in the dermal layer of WT specimens (Figure 4B). The marked augmentation of the contact sensitivity response seen by Bid KO mice could not be explained by a difference in LC density in this mutant strain (Figure 4C). Examination of untreated epidermal sheets from age-matched Bid KO and WT mice revealed no significant difference in LC densities and numbers were consistent with previously published values for B6 mice (WT: 675 / mm^2 ± SE 143, Bid KO: 668 /mm^2 ± SE 178) (35). Neither could it be explained by a difference in LC migration rate or LC culture viability. We examined the numbers of LCs, identified as Langerin positive cells, that migrated from WT and Bid KO skin cultures and their viability over time and found no significant differences (Figure 4D, E).

Enhanced responses by normal naïve transgenic T cells transferred into Bid KO mice

Because T cells have been shown to utilize the Type I pathway of apoptosis by extrinsic signals, the increased immune response seen in Bid KO mice was not likely to be due to aberrant Bid KO T cell proliferation. However, the dynamic expression patterns of Bid in cells and tissues have not been fully characterized. Therefore, to rule out a role for aberrant T cell responses in Bid mice, we directly tested the response of naïve WT T cells to topical immunization in Bid KO and WT mice in adoptive transfer experiments. The protein antigen ovalbumin (OVA) or PBS was painted on tape-stripped ears and thereafter approximately one million CFSE-labeled OT-2 transgenic CD4 T cells were injected *i.v.* via tail vein. Proliferation (reduction in CFSE staining) of OT-2 T cells was examined on day 3 from draining auricular lymph nodes (Figure 5A). No significant differences in weight or cell numbers were seen in the lymph nodes or spleens from PBS control treated WT and Bid KO mice but modest increases were noted for immunized Bid KO spleen (Table I). While both strains supported an efficient response by topical immunization, OT-2 T cell expansion was 1.46-fold greater in Bid KO mice (WT 2.6% ± 0.3 versus Bid KO 3.8% ± 0.2; P < 0.003) (Figure 5A) and a significant increase in the number of T cells that divided 7 times was detected in draining lymph nodes (WT 15% ± 3.1 versus Bid KO 26% ± 2.2; P < 0.05) (Figure 5B). Further, a significant increase in the number of OT-2 T cells that had divided and exited to the periphery was also detected in spleen from Bid KO mice (WT 33% ± 1.8 versus Bid KO 59% ± 3.3, P<0.001) (Figure 5C). The accumulation of dividing cells in lymph node and spleen suggest that Bid KO mice do not induce abortive activation of OT-2 T cells (36). Further, these results suggest that enhanced T cell responsiveness from Bid KO mice may not be due to aberrant T cell proliferation, but due to mechanisms that activate normal T cells.

Bid KO LCs are resistant to CD4 T cell-mediated apoptosis in vitro

To directly test whether Bid KO LCs are apoptosis resistant, migratory cDCs were cultured from the ear skin of both strains in the presence of OVA and subsequently co-cultured with OT-2 or irrelevant 3A9 CD4 T cells overnight. Apoptosis staining was examined by flow cytometry and gated on double positive cells for CD11c and DEC-205, and the LC population was identified as Langerin positive. (The LC-specific antibody used reacts with Langerin molecules on the cell surface, and stained 95% of the gated population) (Figure

6A). We found that the viability of LC after 2-day culture for all samples was 75%, indicating the inevitable fate of death based on intrinsic signals (11). However the hastening of LC death by extrinsic T cell-derived signals was demonstrated in cells from WT mice demonstrating both a loss of Langerin positive cells (from 23% to %16) (Figure 6A) and an increase in apoptotic LCs (increasing from 26% to 42% 7-AAD positive cells) detected in cultures with OT-2 T cells. (Figure 6B). In contrast, OT-2 T cells did not affect Bid KO LC viability since both the percent of Langerin positive cells and viability of LCs was similar to cultures with 3A9 T cells (Figure 6B). In spite of the difference in susceptibility to apoptosis, LCs from both strains supported maximal activation of OT-2 T cells (Figure 6C). A slight increase in the percentage of large (by FALS) CD69 positive T cells was observed (59% versus 65% for OT-2 T cells activated by WT versus Bid KO LCs, respectively). No activation of irrelevant 3A9 CD4 T cells was detected. Resistance to T cell-mediated, antigen-specific apoptosis was consistently observed in Bid KO cDCs (Table II). These results suggest that part of the mechanism for enhanced T cell responsiveness in vivo may due to an increased duration of antigen presenting function by apoptosis-resistant Bid KO cDCs.

Cutaneous dendritic cells from Bid KO mice promote enhanced antigen presentation function upon transfer to WT mice

To determine the contribution of the augmented immune response by cutaneous DCs (cDCs), as opposed to contributing factors from other tissues and cells in Bid KO mice, we isolated migratory cDCs (comprising LCs and dermal (d) DCs) from WT and Bid KO skin explant cultures and tested their stimulatory capacity in adoptive transfer experiments. WT mice containing transferred CFSE-labeled OT-2 T cells were inoculated with equivalent numbers of OVA-pulsed Bid KO or WT migratory cells into WT recipient foot pads. All I-A positive cells expressed both CD11c and CD205 (data not shown). Draining popliteal lymph nodes from OVA-pulsed Bid KO cDCs were 1.8-fold larger than those obtained from OVA-pulsed WT cDCs (233 ± 44 μg/gm mouse weight versus 129 ± 14 μg/gm mouse weight, respectively; P<0.05). Flow cytometric analysis revealed that CD4 T cell proliferation responses were antigen-specific, observed only in CFSE stained cells that were TCR Vβ5 positive (Figure 7A). OT-2 cells responded to OVA-pulsed Bid KO cDCs with both an increase in the rate, as indicated by the faction of cells that divided 5 or more times (28 ± 2.7 % for Bid KO versus 13 ± 0.3% for WT; P<0.05) and the total number of T cells that responded, as indicated by the percent of CD69 positive OT-2 cells in non-dividing fraction plus the percent of proliferating cells (93 ± 0.3% for Bid KO vs 86 ± 0.1% for WT; P<0.001) (Figure 7C). Surprisingly, in this particular experiment, fewer I-A positive cDCs comprised the population of migratory cells from the Bid KO cultures as compared to WT cultures (58% versus 80%, respectively with equivalent mean fluorescence channels; data not shown), indicating that Bid KO cDCs were highly potent antigen presenting cells. (The yield of migratory cDCs (I-A, CD11c and Langerin positive) obtained from each mouse strain differed within some experiments, but these differences revealed no statistically significant trend when all experiments were analyzed.). To correlate increased proliferation with effector function, we examined expanded lymph node and splenic OT-2 T cells for Th1 and Th2 cytokine secretion. Again, draining lymph nodes from Bid KO cDC injected mice were significantly larger and demonstrated greater expansion of CD45.1 OT-2 T cells than control mice (Figures 8A, C). The percent of IFNγ secreting OT-2 cells was modestly increased in lymph node cells but dramatically increased in restimulation cultures of spleen cells from Bid KO cDC injected mice (Figure 8B, E) as compared to control mice. IL-4 secretion was not detectable for any of the immunization regimes. These results show that increased numbers of mature Th1 effector cells are induced by Bid KO cDCs within WT recipients. Thus, enhanced T cell responses did not require the environment of the Bid KO mouse, but was intrinsic to the function of Bid KO cDCs.

Discussion

The results from this study support the hypothesis that an additional layer of immune regulation occurs after successful antigen presentation by LCs to antigen-specific CD4 T cells. During the successful interaction with LCs, T cells provide signals for further activation of LCs ((6) and unpublished results) and subsequent induction of LC apoptosis. The death of incoming LCs may be part of a mechanism for lymph node cells to sense the peripheral load of antigen and may serve to disperse LC-incorporated antigen to endogenous lymph node DC subsets for cross presentation. This CD4 T cell-mediated apoptosis of LCs occurs via Type II apoptotic signals, requiring the BH3-only domain protein Bid, for linking extrinsic death receptor signals to mitochondrial mechanisms of apoptosis. The physiological significance of this observation is demonstrated by the markedly enhanced capacity to augment antigen-specific T cell function in vivo. This was observed for multiple protocols of epicutaneous immunization in Bid KO mice, or by inoculation of cutaneous DC from antigen painted Bid KO mice into WT recipients. Thus, the data suggest that the longevity of activated, antigen-pulsed LCs in vivo directly correlates with the magnitude of the immune response that can be generated.

We found that peptide inhibitors for Caspase 8 or 9 could only partially inhibit T cell-mediated LC apoptosis, while pan caspase or "effector" caspase 3 inhibitors almost completely blocked LC apoptosis. The inability to completely inhibit "initiator" caspases 8 and 9 may due to a number of reasons: 1) The amount of caspase protein may be too high to allow saturation by the inhibitor peptide at the concentrations used, 2) the caspases may be molecularly sequestered from inhibitory effects of the peptide, or 3) for caspase 9, the Type I or II apoptosis pathway used may not be absolute. In the later case, perhaps both pathways may be used simultaneously in the same cell, or used independently in different LC subsets depending on their interaction with the T cell. Therefore, the classification of LC as a Type II cell, by this criterion may not be strictly applied. Nevertheless, the Type II cascade is in place within LC, supported by our finding that high levels of the Bid protein is expressed in our LC line and specifically activated after antigen-specific T cell interaction. Furthermore, the role of Bid in primary LC was studied in Bid KO mice, and the data from those studies indicate that if compensatory Type I pathway is used by LC it is not complete. Thus, taken together, these data support our hypothesis that there is a preference for the use of the Type II cascade in CD4 T-cell mediated LC apoptosis.

Our results are consistent with a number of studies that have identified a critical role for the Bcl-2 family genes, *bcl-x_L* and *bcl-2* in maintaining DC longevity. However, studies on the impact of Bcl-2 family gene transfection do not indicate whether intrinsic, extrinsic or both apoptotic pathways are affected. DCs from CD11c-promoter-driven *bcl-2* transgenic mice display increased longevity in vitro and in vivo, and induce augmented immune responses when transferred into WT recipients (37). Activated T cells secrete TNF-related activation-induced cytokine (TRANCE) and express CD40L, molecules that have been shown to improve survival of cultured bone-derived or splenic DCs, and correlate with an increase in Bcl-x_L and Bcl-2 expression, respectively (38, 39). Whether cutaneous DCs or LCs are similar to conventional DCs in response to TRANCE or CD40L needs be addressed. While our studies indicate LCs undergo cell death after prolonged interaction with antigen-specific T cells, these observations do not exclude a role for TRANCE- and CD40L-induced survival signals early during T cell interaction – promoting prolonged cell-cell contact that is required for successful CD4 T cell activation and differentiation (40, 41). Alternatively, different DC subsets may respond differently to activated T cell signals and cytokines. Other studies using gene gun-mediated DNA-based vaccines suggest that cutaneous DCs do rely on *bcl-x_L* and *bcl-2* gene expression for generating or enhancing such cutaneous vaccines (42, 43). Our studies support and extend those studies, showing that the mitochondrial

pathway is essential for mediating extrinsic activation-induced apoptosis signals from antigen-specific T cells, and that it is Bid-dependent.

The nature of the extrinsic signal(s) provided by T cells is currently under investigation. While it is known that antigen bearing LCs from *lpr*-mutant (Fas null) mice demonstrate increased longevity (44) and resist apoptosis in vivo after hapten (FITC) painting or in a graft versus host disease model (7), we have been unsuccessful in blocking in vitro T cell-mediated apoptosis of LCs using neutralizing agents for either FasL or TNF-related apoptosis-inducing ligand (TRAIL) (data not shown, manuscript in preparation). This may indicate that either the LC-T cell interface may be impenetrable to such soluble neutralizing agents, or that other mediators of apoptosis are involved and remain to be identified.

Very little is known regarding Bid expression and utilization in normal tissues. A limited immunohistochemical survey was done using anti-Bid sera (45). The strongest staining was detected in neuronal cells, stratified squamous epithelium and in short-lived leukocytes (germinal center cells, granulocytes, macrophages), while monocytes, immature bone-marrow cells and cortical thymocytes were reported as negative. This is consistent with our inability to detect significant Bid protein levels in splenic T cells or T hybridoma lines . Definitive studies on the expression of Bid in DC subsets have not been performed. Thus, this is the first demonstration that a DC subset, specifically LCs, expresses and activates Bid in response to extrinsic apoptotic stimuli. Investigations of the expression and utilization of Bid by different DC subsets in response to various stimuli are currently underway.

Because Bid has also been detected in differentiated squamous keratinocytes (45), we considered that there may be aberrations in keratinocyte biology that might contribute to the enhanced ear swelling observed in Bid KO mice. Therefore, we performed histochemical analysis of resting and contact sensitized ear specimens. Extensive pathological examination comparing Bid and WT epidermis revealed normal epidermal morphology in resting tissues. However, while both WT and Bid KO specimens demonstrated a similar influx infiltrating cells affecting the dermal and epidermal layers during the swelling response peak at Day 3, the extended swelling response, seen on Day 5 for Bid KO, when the swelling response diminished for WT, correlated with an increased incidence of infiltrating cells within the epidermis. These findings suggest that prolonged active immunity continued in Bid KO as compared to WT. Alternatively, Bid KO inflammatory cells, reportedly shown to express Bid (ie. granulocytes and macrophages) may also play a role in prolonging the local inflammatory and/or lymphocyte recruitment response due to extended life spans or unresponsive down regulatory mechanisms. However, control vehicle sensitized Bid mice treated with a challenge dose of hapten did not develop swelling responses. This observation indicates that differences in inflammatory mechanisms alone do not contribute to the enhanced contact sensitization response in Bid KO mice. It is likely that multiple components play a role, and further experiments will be needed to address these possibilities.

The complexity of the Bid KO response to topical immunization required that we examine the behavior of cDCs in absence of the Bid KO host environment. Therefore, we harvested migratory cDCs from topically immunized skin explant cultures and examined their capacity to activate normal T cells in a WT host environment. We observed that upon adoptive transfer into WT recipient mice containing CFSE-labeled CD4 T cells, draining lymph nodes from mice inoculated with antigen-pulsed Bid KO cDCs were almost 2-fold larger as compared nodes of mice receiving antigen-pulsed WT cDCs. The cell proliferation that occurred within these enlarged lymph nodes was shown to be antigen specific, since TCR Vβ5 negative CFSE-labeled CD4 T cells, co-transferred into in the same mouse showed no proliferation response. The increased rate and magnitude of the OT-2 T cell proliferation

observed correlated with an increase in Th1 IFNγ producing cells found in both draining lymph nodes and spleen. Thus, Bid KO cDCs, in normal host recipient mice, promote increased effector T cell differentiation, not abortive proliferation.

We recognize that migratory cells from split ear specimens contain CD11c, I-A positive LCs and dDCs derived from both epidermal and dermal layers. Therefore, the effects seen in vivo by cDCs may be contributed by either or both DC populations. We have found that 70 - 90% of I-A+ or CD11c+ cells are also positive for the LC marker Langerin (CD207) (46). To enrich for activated LCs in our in vitro analysis we examined I-A^{high} and/or Langerin expressing cells, both shown to correlate with LC phenotype (46, 47: Takahara, 2002 #344). Therefore, migratory Bid KO-derived cDCs likely comprise mostly LCs (CD11c, CD205, Langerin positive cells). The Bid KO LC population demonstrates resistance to CD4 T cell-induced apoptosis in vitro and supports the hypothesis they may have a longer life span in the lymph node. The lifespan of such apoptosis-resistant LCs (AR-LCs) within the lymph node during the generation of antigen-specific responses will need to be examined to verify this interpretation.

Recent evidence points to the requirement of prolonged CD4-DC interactions, and prolonged presence of antigen to sustain CD4 activation, proliferation (40, 48) and differentiation (41). Thus, an increased lifespan within the LC population may directly impact the duration of productive antigen presentation and sustained CD4 proliferation within the lymph node, allowing a larger number of CD4 T cells to modulate the effector arm of the immune response. Our finding that Bid KO cDCs promote increased numbers of IFNγ positive OT-2 cells supports this hypothesis. The impact of AR-LCs on development of memory and on supporting the generation of CD8 T cell effector and memory cells requires further investigation.

While Bid KO mice are reported to be phenotypically normal(23), detailed analysis of immune system function has not been previously reported. Interestingly, while Bid protein expression is restricted to neurons and to terminally differentiated cells fated to possesses short life spans (45), no increase in the rate of cancer development (including skin) has been documented, with the exception of a profound increase (53% in Bid KO versus 3% in WT) in the incidence of chronic myelomonocytic leukemia (CMML) (49). This phenotype suggests that in young mice Bid-independent compensatory mechanisms exist to regulate tissue and cellular homeostasis, but with age, myeloid lineage cells have greater dependence on the Type II apoptosis pathway for regulating their life span. Alternatively, Bid's other function, controlling cell-cycle checkpoints during replicative stress, may be critical in aged myeloid precursors (50, 51). These observations are consistent with our findings that Bid has a critical role in the biology of myeloid lineage-derived LCs (52), and suggests that other myeloid DC subsets may also utilize the Type II pathway.

The finding that Bid is utilized in a physiologically relevant manner to regulate LC function makes it an attractive molecular target for manipulating immune responses. There are a number of advantages in targeting Bid for such purposes: 1) Selective cell-targeting; DCs and cells with reduced proliferative potential (i.e. terminally differentiated) primarily express Bid. And so far, only LCs (as reported here) and hepatocytes (23) have been shown to utilize the Type II pathway in normal hematopoietic tissues. Although, we expect that with more detailed investigation of the Bid KO strain, other cells may demonstrate some dependency on Bid for, perhaps, subtle impacts on normal mechanisms of homeostasis. 2) Reduced dysregulation; Bid KO cells can still respond to intrinsic and extrinsic Type I signals of cell death, hence a normal phenotype is observed in Bid KO mice. 3) T cells unaffected: Bid-restricted expression spares T cells if systemic inhibitors were employed. 4) Inhibition time frame is short; Only short-term inhibition during antigen presentation is

required to be effective in enhancing an immune response. Therefore, we propose that Bid-specific inhibitors may be therapeutically used as potent augmenters of "engineered" immune responses.

Acknowledgments

3 Abbreviations used

7-AAD	7-amino-actinomycin D
AR-LCs	apoptosis-resistant LCs
cDC	cutaneous DC
CFSE	carboxyfuoroscein diacetate succinimidyl ester
dDC	dermal DC
DNFB	dinitrofluorobenzene
HEL	hen egg lysozyme
LC	Langerhans cell
OVA	chicken ovalbumin

References

1. Bancherau J, Steinman RM. Dendritic cells and the control of immunity. Nature. 1998; 392:245–252. [PubMed: 9521319]

2. Bancherau J, Briere F, Caux C, Davoust J, Lebecque S, Liu YJ, Pulendran B, Palucka K. Immunobiology of dendritic cells. Annual Review of Immunology. 2000; 18:767–811.

3. Steinman RM, Hawiger D, Liu K, Bonifaz L, Bonnyay D, Mahnke K, Iyoda T, Ravetch J, Dhodapkar M, Inaba K, Nussenzweig M. Dendritic cell function in vivo during the steady state: a role in peripheral tolerance. Annals of the New York Academy of Sciences. 2003; 987:15–25. [PubMed: 12727620]

4. Larrengina AT, Falo LD. Changing paradigms in cutaneous immunology: adapting with dendritic cells. Journal of Investigative Dermatology. 2005; 124:1–12. [PubMed: 15654947]

5. Sallusto F, Cella M, Danieli C, Lanzavecchia A. Dendritic cells use macropinocytosis and the mannose receptor to concentrate macromolecules in the major histocompatibility complex class II compartment: downregulation by cytokines and bacterial products. Journal of Experimental Medicine. 1995; 182:389–400. [PubMed: 7629501]

6. Kitajima T, Caceres-Dittmar G, Tapia FJ, Jester J, Bergstresser PR, Takashima A. T cell-mediated terminal maturation of dendritic cells: loss of adhesive and phagocytotic capacities. Journal of Immunology. 1996; 157:2340–2347.

7. Merad M, Hoffmann P, Ranheim E, Slaymaker S, Manz MG, Lira SA, Charo I, Cook DN, Weissman IL, Strober S, Engleman EG. Depletion of host Langerhans cells before transplantation of donor alloreactive T cells prevents skin graft-versus-host disease. Nature Medicine. 2004; 10:510–517.

8. Kamath AT, Pooley J, O'Keeffe MA, Vremec D, Zhan Y, Lew AM, D'Amico A, Wu L, Tough DF, Shortman K. The development, maturation, and turnover rate of mouse spleen dendritic cell populations. Journal of Immunology. 2000; 165:6762–6770.

9. Kamath AT, Henri S, Battye F, Tough DF, Shortman K. Developmental kinetics and lifespan of dendritic cells in mouse lymphoid organs. Blood. 2002; 100:1734–1741. [PubMed: 12176895]

10. Ingulli E, Mondino A, Khoruts A, Jenkins MK. In vivo detection of dendritic cell antigen presentation to CD4(+) T cells. Journal of Experimental Medicine. 1997; 185:2133–2141. [PubMed: 9182685]

11. Hou W-S, Parijs LV. A Bcl-2-dependent molecular timer regulates the lifespan and immunogenicity of dendritic cell. Nature Immunology. 2004; 5:583–589. [PubMed: 15133508]

12. Langenkamp A, Messi M, Lanzavecchia A, Sallusto F. Kinetics of dendritic cell activation: impact on priming of TH1, TH2 and nonpolarized T cells. Nature Immunology. 2000; 1:311–316. [PubMed: 11017102]

13. Matsue H, Edelbaum D, Hartmann AC, Morita A, Bergstresser PR, Yagita H, Okumura K, Takashima A. Dendritic cells undergo rapid apoptosis in vitro during antigen-specific interaction with CD4+ T cells. Journal of Immunology. 1999; 162:5287–5298.

14. Ashany D, Savir A, Bhardwaj N, Elkon KB. Dendritic cells are resistant to apoptosis through the Fas (CD95/APO-1) pathway. Journal of Immunology. 1999; 163:5303–5311.

15. Scaffidi C, Fulda S, Srinivasan A, Friesen C, Li F, Tomaselli KJ, Debatin KM, Krammer PH, Peter ME. Two CD95 (APO-1/Fas) signaling pathways. EMBO Journal. 1998; 17:1675–1687. [PubMed: 9501089]

16. Opferman JT, Korsmeyer SJ. Apoptosis in the development and maintenance of the immune system. Nature Immunology. 2003; 4:410–415. [PubMed: 12719730]

17. Danial NN, Korsmeyer SJ. Cell death: critical control points. Cell. 2004; 116:205–219. [PubMed: 14744432]

18. Korsmeyer SJ, Wei MC, Saito M, Weiler S, Oh KJ, Schlesinger PH. Pro-apoptotic cascade activates BID, which oligomerizes BAK or BAX into pores that result in the release of cytochrome c. Cell Death & Differentiation. 2000; 7:1166–1173. [PubMed: 11175253]

19. Lundqvist A, Nagata T, Kiessling R, Pisa P. Mature dendritic cells are protected from Fas/CD95-mediated apoptosis by upregulation of Bcl-X(L). Cancer Immunology, Immunotherapy. 2002; 51:139–144.

20. Pirtskhalaishvili G, Shurin GV, Gambotto A, Esche C, Wahl M, Yurkovetsky ZR, Robbins PD, Shurin MR. Transduction of dendritic cells with Bcl-xL increases their resistance to prostate cancer-induced apoptosis and antitumor effect in mice. Journal of Immunology. 2000; 165:1956–1964.

21. Nopora A, Brocker T. Bcl-2 controls dendritic cell longevity in vivo. Journal of Immunology. 2002; 169:3006–3014.

22. Kim TW, Lee JH, He L, Boyd DA, Hung CF, Wu TC. DNA vaccines employing intracellular targeting strategies and a strategy to prolong dendritic cell life generate a higher number of CD8+ memory T cells and better long-term antitumor effects compared with a DNA prime-vaccinia boost regimen. Human Gene Therapy. 2005; 16:26–34. [PubMed: 15703486]

23. Yin XM, Wang K, Gross A, Zhao Y, Zinkel S, Klocke B, Roth KA, Korsmeyer SJ. Bid-deficient mice are resistant to Fas-induced hepatocellular apoptosis. Nature. 1999; 400:886–891. [PubMed: 10476969]

24. Ho WY, Cooke MP, Goodnow CC, Davis MM. Resting and anergic B cells are defective in CD28-dependent costimulation of naive CD4+ T cells. J. Exp. Med. 1994; 179:1539–1549. %R 10.1084/jem.179.5.1539. [PubMed: 7909325]

25. Xu S, Bergstresser PR, Takashima A. Phenotypic and functional heterogeneity among murine epidermal-derived dendritic cell clones. Journal of Investigative Dermatology. 1995; 105:831–836. [PubMed: 7490479]

26. Timares L, Takashima A, Johnston SA. Quantitative analysis of the immunopotency of genetically transfected dendritic cells. Proceedings of the National Academy of Sciences of the United States of America. 1998; 95:13147–13152. [PubMed: 9789056]

27. Timares L, Douglas JT, Tillman BW, Krasnykh V, Curiel DT. Adenovirus-mediated gene delivery to dendritic cells. Methods in Molecular Biology. 2004; 246:139–154. [PubMed: 14970589]

28. Wu X, Wakefield JK, Liu H, Xiao H, Kralovics R, Prchal JT, Kappes JC. Development of a novel trans-lentiviral vector that affords predictable safety. Molecular Therapy: the Journal of the American Society of Gene Therapy. 2000; 2:47–55. [PubMed: 10899827]

29. Chen W, Wu X, Levasseur DN, Liu H, Lai L, Kappes JC, Townes TM. Lentiviral vector transduction of hematopoietic stem cells that mediate long-term reconstitution of lethally irradiated mice. Stem Cells. 2000; 18:352–359. [PubMed: 11007919]

30. Allen PM, Matsueda GR, Haber E, Unanue ER. Specificity of the T cell receptor: two different determinants are generated by the same peptide and the I-Ak molecule. Journal of Immunology. 1985; 135:368–373.

31. Ortner U, Inaba K, Koch F, Heine M, Miwa M, Schuler G, Romani N. An improved isolation method for murine migratory cutaneous dendritic cells. Journal of Immunological Methods. 1996; 193:71–79. [PubMed: 8690932]

32. Timares L, Safer KM, Qu B, Takashima A, Johnston SA. Drug-inducible, dendritic cell-based genetic immunization. Journal of Immunology. 2003; 170:5483–5490.

33. Yague J, White J, Coleclough C, Kappler J, Palmer E, Marrack P. The T cell receptor: the alpha and beta chains define idiotype, and antigen and MHC specificity. Cell. 1985; 42:81–87. [PubMed: 2410143]

34. Xu H, DiIulio NA, Fairchild RL. T cell populations primed by hapten sensitization in contact sensitivity are distinguished by polarized patterns of cytokine production: interferon gamma-producing (Tc1) effector CD8+ T cells and interleukin (Il) 4/Il-10-producing (Th2) negative regulatory CD4+ T cells. Journal of Experimental Medicine. 1996; 183:1001–1012. [PubMed: 8642241]

35. Bergstresser PR, Fletcher CR, Streilein JW. Surface densities of Langerhans cells in relation to rodent epidermal sites with special immunologic properties. The Journal Of Investigative Dermatology. 1980; 74:77. [PubMed: 6985948]

36. Mayerova D, Parke EA, Bursch LS, Odumade OA, Hogquist KA. Langerhans cells activate naive self-antigen-specific CD8 T cells in the steady state. Immunity. 2004; 21:391–400. [PubMed: 15357950]

37. Nopora A, Brocker T. Bcl-2 Controls Dendritic Cell Longevity In Vivo. J Immunol %R. 2002; 169:3006–3014.

38. Wong BR, Josien R, Choi Y. TRANCE is a TNF family member that regulates dendritic cell and osteoclast function. Journal of Leukocyte Biology. 1999; 65:715–724. [PubMed: 10380891]

39. Koppi TA, Tough-Bement T, Lewinsohn DM, Lynch DH, Alderson MR. CD40 ligand inhibits Fas/CD95-mediated apoptosis of human blood-derived dendritic cells. European Journal of Immunology. 1997; 27:3161–3165. [PubMed: 9464801]

40. Obst R, van Santen H, Mathis D, Benoist C. Antigen persistence is required throughout the expansion phase of a CD4(+) T cell response. J Exp Med. 2005; 201:1555–1565. [PubMed: 15897273]

41. Hurez V, Saparov A, Tousson A, Fuller MJ, Kubo T, Oliver J, Weaver BT, Weaver CT. Restricted clonal expression of IL-2 by naive T cells reflects differential dynamic interactions with dendritic cells. Journal of Experimental Medicine. 2003; 198:123–132. [PubMed: 12835480]

42. Kim TW, Hung CF, Ling M, Juang J, He L, Hardwick JM, Kumar S, Wu TC. Enhancing DNA vaccine potency by coadministration of DNA encoding antiapoptotic proteins.[see comment]. Journal of Clinical Investigation. 2003; 112:109–117. [PubMed: 12840065]

43. Hon H, Rucker EB 3rd, Hennighausen L, Jacob J. bcl-xL is critical for dendritic cell survival in vivo. Journal of Immunology. 2004; 173:4425–4432.

44. Kawamura T, Azuma M, Kayagaki N, Shimada S, Yagita H, Okumura K. Fas/Fas ligand-mediated elimination of antigen-bearing Langerhans cells in draining lymph nodes. British Journal of Dermatology. 1999; 141:201–205. [PubMed: 10468788]

45. Krajewska M, Zapata JM, Meinhold-Heerlein I, Hedayat H, Monks A, Bettendorf H, Shabaik A, Bubendorf L, Kallioniemi OP, Kim H, Reifenberger G, Reed JC, Krajewski S. Expression of Bcl-2 family member Bid in normal and malignant tissues. Neoplasia (New York). 2002; 4:129–140.

46. Takahara K, Omatsu Y, Yashima Y, Maeda Y, Tanaka S, Iyoda T, Clausen BE, Matsubara K, Letterio J, Steinman RM, Matsuda Y, Inaba K. Identification and expression of mouse Langerin (CD207) in dendritic cells. International Immunology. 2002; 14:433–444. [PubMed: 11978773]

47. Kissenpfennig A, Henri S, Dubois B, Laplace-Builhe C, Perrin P, Romani N, Tripp CH, Douillard P, Leserman L, Kaiserlian D, S. S, Davoust J, Malissen B. Dynamics and function of Langerhans cells in vivo dermal dendritic cells colonize lymph node areas distinct from slower migrating Langerhans cells. Immunity. 2005; 22:643–654. [PubMed: 15894281]

48. Gett AV, Sallusto F, Lanzavecchia A, Geginat J. T cell fitness determined by signal strength. Nature Immunology. 2003; 4:355–360. [PubMed: 12640450]

49. Zinkel SS, Ong CC, Ferguson DO, Iwasaki H, Akashi K, Bronson RT, Kutok JL, Alt FW, Korsmeyer SJ. Proapoptotic BID is required for myeloid homeostasis and tumor suppression. Genes & Development. 2003; 17:229–239. [PubMed: 12533511]

50. Kamer I, Sarig R, Zaltsman Y, Niv H, Oberkovitz G, Regev L, Haimovich G, Lerenthal Y, Marcellus RC, Gross A. Proapoptotic BID is an ATM effector in the DNA-damage response. Cell. 2005; 122:593–603. [PubMed: 16122426]

51. Zinkel SS, Hurov KE, Ong C, Abtahi FM, Gross A, Korsmeyer SJ. A role for proapoptotic BID in the DNA-damage response. Cell. 2005; 122:579–591. [PubMed: 16122425]

52. Ginhoux F, Tacke F, Angeli V, Bogunovic M, Loubeau M, Dai XM, Stanley ER, Randolph GJ, Merad M. Langerhans cells arise from monocytes in vivo. Nature Immunology. 2006; 7:265–273. [PubMed: 16444257]
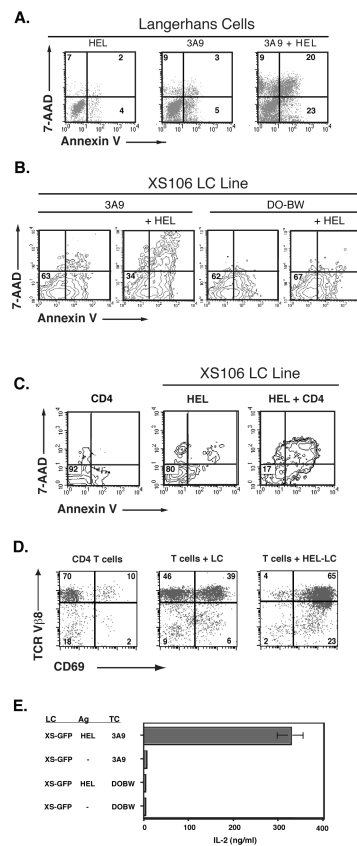
Figure 1. T cell-mediated apoptosis of LCs or XS106 LC lines by antigen-specific T cells
A. Langerhans cells are susceptible to CD4 T cell-mediated apoptosis. LCs were isolated from the supernatant of two day mouse ear skin organ cultures. LCs were further cultured overnight in 100ng/ml hen egg lysozyme (HEL) protein and / or 3A9 T hybridoma at a ratio of 1:4 LC:TC. Cultured samples were stained with FITC–anti-I-Ak (2G9), PE–Annexin V and 7-AAD (5µg/ml). The uptake of vitally excluded dye 7-AAD was measured by flow cytometry as an indicator of later stages of death and Annexin V staining as an early indicator of apoptosis. Three-color flow cytometric analysis of PE– Annexin V and 7-AAD staining was performed on FITC–I-Ak positive gated cells. B. Antigen-specific T cell - induced apoptosis in XS106 cells. GFP positive clone XS106 B1.1 cells were incubated with or without HEL protein (1 mg/ml) overnight then mixed with T hybridoma cells specific for HEL (3A9) or irrelevant OVA (DO-BW) antigens at a ratio of 1:4 LC:TC and cultured overnight. GFP positive XS106 were gated and analyzed for PE-Annexin V and 7-AAD staining by flow cytometry and the results displayed in contour map. C. Naïve CD4 splenocytes from 3A9 transgenic mice induce significant apoptosis in XS106 cells. XS106 cells were incubated with HEL protein (1 mg/ml) overnight then mixed with purified CD4 3A9 splenocytes specific for HEL (3A9) at a ratio of 1:5 LC:TC and cultured overnight. CD4 T cell and LC populations were gated by large size (light scatter properties). CD4 cells alone, HEL-pulsed XS106 alone, or the mix of CD4 + HEL pulsed XS106 were analyzed for PE-Annexin V and 7-AAD staining by flow cytometry. Numbers indicate the percent of gated cells within that quadrant. Lower left quadrant contains viable cells.
D. Naive T cells respond to XS106 antigen presentation. Purified naïve splenic CD4 T cells from 3A9 transgenic mice were mixed with LCs (XS106 cells) and co-culture for 20 hours in the presence or absence of HEL (100 µg/ml). Small and blast T cells were easily distinguished from large XS106 and gated by light scatter properties for analysis of CD69

and TCR expression. The percent of T cells in each quadrant is shown in each quadrant. E. IL-2 production from antigen-specific T cell hybridoma, 3A9. XS-GFP cells were pre-pulsed with or without HEL protein (1 mg/ml) overnight, then mixed with HEL-3A9 specific or irrelevant OVA-specific DO-BW T hybridoma cells at a ratio of 1:4 LC:TC and cultured for another 20 hours. T hybridoma activation was tested by detecting IL-2 in the culture supernatants by ELISA.
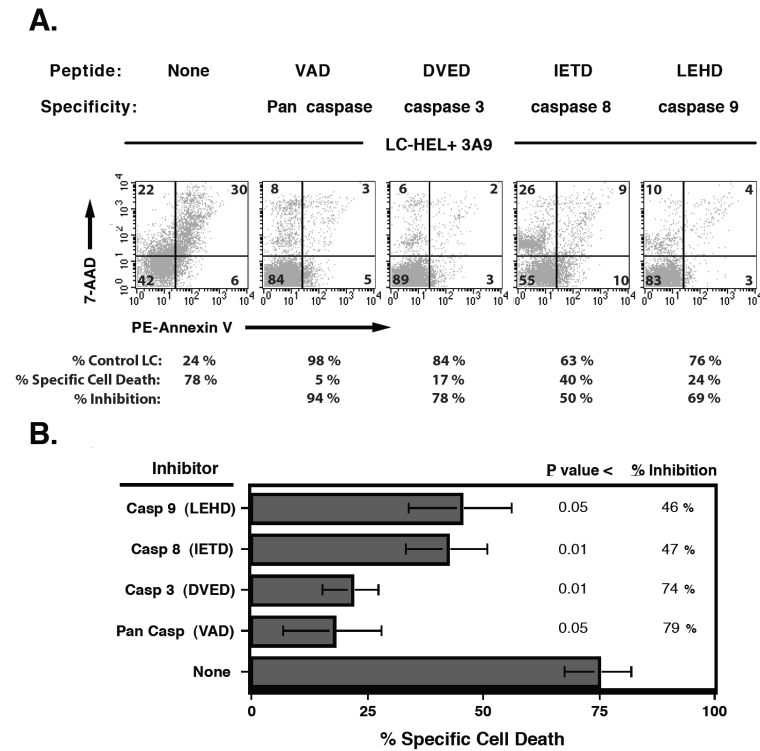
A.

Peptide:	None	VAD	DVED	IETD	LEHD
Specificity:		Pan caspase	caspase 3	caspase 8	caspase 9

LC-HEL+ 3A9

7-AAD →

PE-Annexin V →

% Control LC:	24 %	98 %	84 %	63 %	76 %
% Specific Cell Death:	78 %	5 %	17 %	40 %	24 %
% Inhibition:		94 %	78 %	50 %	69 %

B.

Inhibitor	P value <	% Inhibition
Casp 9 (LEHD)	0.05	46 %
Casp 8 (IETD)	0.01	47 %
Casp 3 (DVED)	0.01	74 %
Pan Casp (VAD)	0.05	79 %
None		

% Specific Cell Death

Figure 2. Caspase inhibition of T cell-induced apoptosis of the LC line XS106
A. GFP positive XS106 B1.1 cells analyzed for apoptosis by PE-Annexin V and 7AAD staining. XS106 B1.1 cells were pulsed with or without HEL antigen overnight and mixed with either 3A9 T cells or unlabeled XS106 as a control. One hour prior to mixing cells they were preincubated with the following caspase inhibitors: Z-VAD-FMK 100μM, Z-DEVD-FMK 200μM, Z-IETD-FMK 150μM and Ac-LEHD-CHO 300μM and then continuously cultured in the presence of these inhibitors. Apoptosis levels were assessed after 16 -20 hours by flow cytometry. GFP positive XS106 B1.1 were gated and analyzed for apoptosis by PE-Annexin V and 7AAD staining. The listed % Control LC values indicate the background-adjusted percent of remaining XS106 B1.1cells . B. % Inhibition summary. The average ± SEM from 4 independent experiments. (see Materials and Methods for calculations).
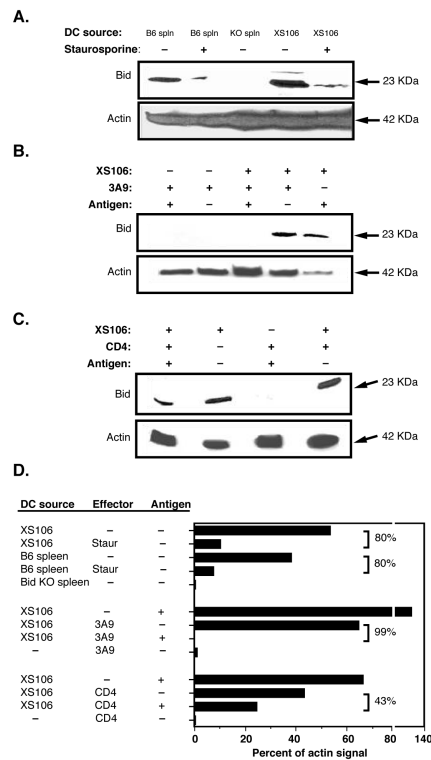
Figure 3. Bid activation in DC upon antigen specific interaction with T-cells

A. Bid activation in DC. To test Langerhans cell Bid cleavage, we utilized staurosporine-induced release of cytochrome c, which induces caspase 3 mediated Bid cleavage. Cells were cultured overnight with or without Staurosporine (500 nM). Cell lysate was obtained and 100 micrograms of protein was loaded per sample and analyzed by Western blot with the indicated antibody. Spleen cells from Bid KO mice are loaded as a control. B. Ag-specific T-cell mediated activation of Bid cleavage by 3A9 Hybridoma T cells. T cells were mixed 4:1 with DC pulsed or unpulsed with HEL antigen. Protein lysates from half of the indicated culture was loaded for each sample (~ 100 micrograms) and analyzed by Western blot. C. Splenic naïve CD4 T cells induce Bid cleavage in DC. CD4 T cells purified from 3A9 transgenic mice were mixed 4:1 with DC pulsed with or without HEL antigen. Half of the total cell culture input was loaded (~50μg). D. Densitometry of Bid as a percentage of actin band intensities quantifies the level of Bid activation. Values indicate the percent loss of Bid intensity (and therefore activation) as compared to paired controls.
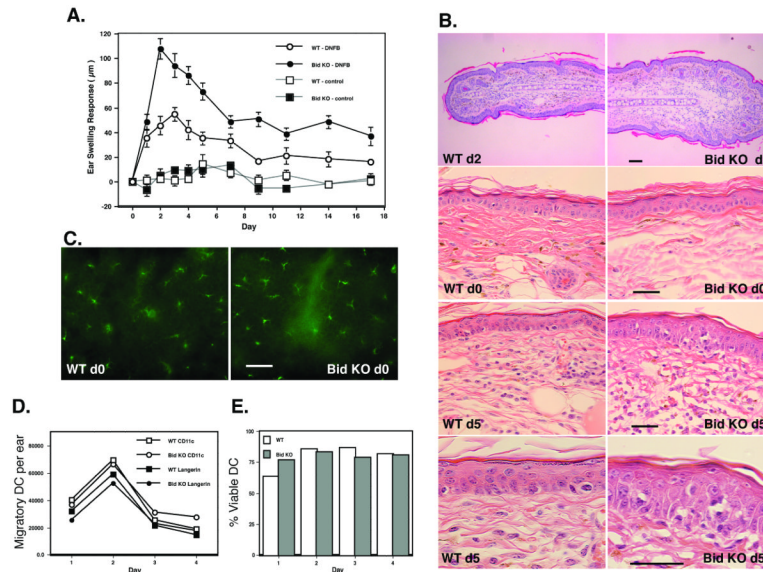
Figure 4. Enhanced contact sensitization in Bid null mice
A. Kinetics of the swelling response. Four age-matched mice per group of WT or Bid KO were sensitized with vehicle only or 0.5% DNFB on the stomach and paws of each mouse. On Day 5 base line measurement of ear thickness was taken for each ear. Mice were subsequently challenged with 0.2% DNFB applied on dorsal and ventral sides of the ears (Day 0 is day of challenge). Ear thickness measurements were taken thereafter on the following days, as shown. Ear thickness shown are that over baseline measurements for each ear. All significant differences are noted in the following manner: * = p< 0.05, **= p< 0.01, *** = p< 0.001. This is representative of 3 similar experiments. B. Histological comparison of WT and Bid epidermal sections. Parafin-embedded sections of ear specimens obtained on Day 0 and Day 5 post hapten challenge were stained by H&E. Magnifications of 10x upper panel, 20x middle pannals and 40x in lower panel are shown for WT and Bid contact sensitized ears. The bar length indicates 100 μM. C. Langerhans cell densities are equivalent in Bid null and WT mice. Whole mounts of epidermal sheets from age matched Bid KO and WT mice were stained with FITC-anti MCH class II, or isotype control (data not shown) and examined by fluorescence microscopy. Digital images at 20x magnification and the number of MHC class II positive cells was determined. D., E. LC migration and viability are similar for WT and Bid KO cells during ear skin culture. Ear skin samples were prepared for culture after tape stripping six mice per group. Ear skin halves were transferred to fresh wells daily for 4 days. Pooled samples per day of culture were counted, and stained with DC specific antibodies (FITC-CD11c, PE-DEC205, APC-biotin-Langerin, isotype controls) and 7-AAD. Flow cytometry was performed to assess phenotype and viability. D. Migration Kinetics. Total CD11c positive (open symbols) and Langerin positive (closed symbols) cells per ear culture of WT (square) and Bid KO (circle) mice were calculated based on total cell counts and percent positive cells. B. Migratory cell viability. The percent of 7-AAD negative, CD11c positive cells migrated from ear skin samples from each day are shown. The total viable LC yields from WT (1.27×10^5) and Bid KO (1.20×10^5) ears were similar.
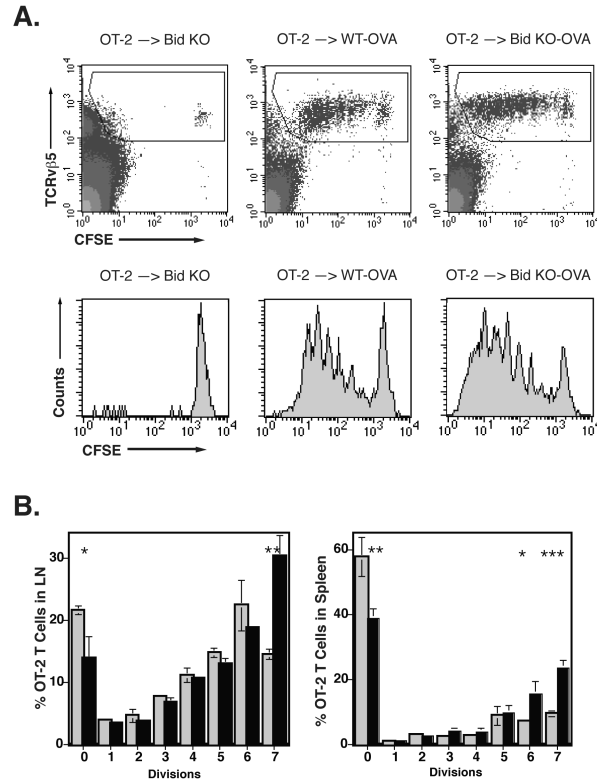
Figure 5. Enhanced OT-2 T cell responses in Bid null mice

WT and Bid KO mice were topically immunized by application of 25 µg OVA onto tape-stripped ear surfaces. CD4 purified CFSE labeled OT-2 cells (1.5×10^6) were injected into topically immunized mice via tail vein. Draining lymph node cells and spleen cells were harvested from mice on day 3 and analyzed for dilution of CFSE within the TCR Vβ5 positive population. A. Increased rate of proliferation by OT-2 T cell in Bid mice. CFSE log fluorescence from gated OT-2 cells transferred to control Bid KO (or WT, not shown) mice (left panels), immunized WT mice (middle panels) or immunized Bid KO mice (right panels) are shown. OT-2 gate was set as shown and represented 0.05%, 2.6% and 3.8% of total lymph node cells for immunized Bid KO, WT-OVA and Bid KO-OVA mice, respectively. P<0.003 comparing WT-OVA and Bid KO-OVA responses, n=3. B. Enhanced proliferation and emigration to spleen by OT-2 T cells in Bid KO mice. Lymph nodes (left panel) and spleen (right panel) were harvested from triplicate mice per group. OT-2 cells were analyzed as shown in A and the percent of cells present in each division region, based on fluorescence intensity, was determined. The average value and SEM are shown for each group (light bars for WT, solid bars for Bid KO). P values are represented by asterisks as follows: *, P < 0.05; **, P < 0.01, ***, P < 0.001.
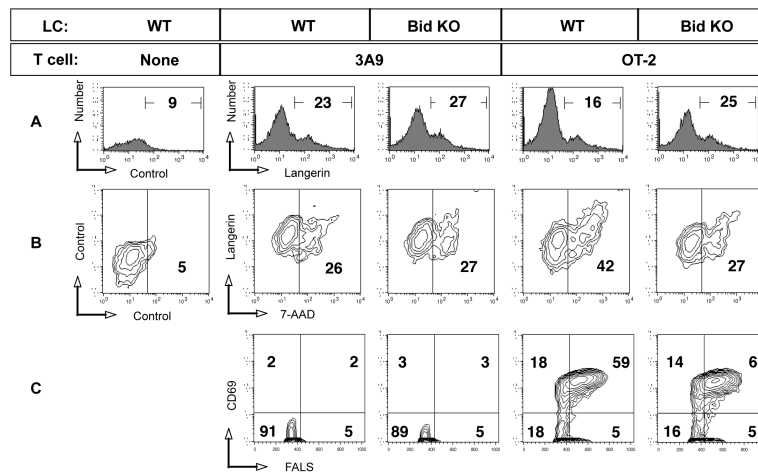
Figure 6. Bid KO LCs are resistant to antigen-specific T cell-mediated apoptosis
cDCs migrated from ear skin in the presence of indicated antigen over 2 days, harvested and mixed with purified OT-2 cells at 1:4 ratio. After 20 hours, cultures were subjected to flow cytometric analysis after staining with fluorochrome-conjugated antibodies and dyes as follows: FITC-CD11c, PE-CD205, 7-AAD, APC-biotin-Langerin. A. The percent of Langerin positive cells is shown, indicating the remaining LCs in each mixed culture. B. Double positive CD11c, CD205 cells were gated and analyzed for Langerin and 7-AAD uptake. Numbers displayed in the right quadrant indicate the percent 7-AAD positive cells. C. Cells falling in the small lymphocyte gate based on light scatter properties were examined for early activation marker CD69, with percentage of positive cells displayed. One of 3 similar experiments.
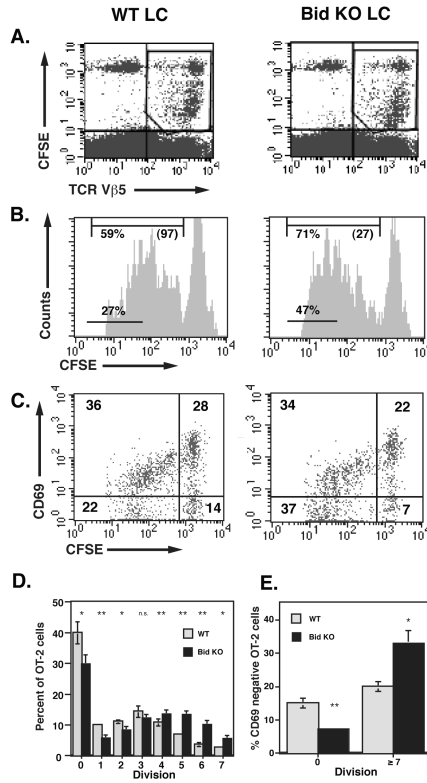
Figure 7. Inoculated Bid KO cDCs promote augmented T cell activation in vivo
Bid KO and WT mouse ears were tape-stripped and painted with 25μg OVA or HEL in
PBS. After an hour, mice were sacrificed and ear specimens harvested for explant culture.
Migratory cDCs were cultured from specimens over 48 hours in the presence of OVA
(100μg/ml) or HEL (100μg/ml). One million CFSE-labeled CD4 OT-2 T cells were injected
via tail vein to WT mice (In this experiment, 50% of the CFSE labeled CD4 cells were OT-2
TCR negative, as indicated by absence of TCR Vβ5 staining - and served as an internal
specificity control) and cDCs (5×10^4) were inoculated into the footpad the same day.
Popliteal lymph nodes were harvested from individual mice (3 per group) and weighed
before processing for TCR and CD69 staining. Flow cytometric analysis plots of (A) the
gate used for CFSE-TCR Vβ5 cells, (B) the level of CFSE dilution (indicating cell
divisions) and (C) the level of T cell activation/maturation-indicated by transient CD69 up
then down regulation are shown. (D) Significant differences in the rate of proliferation
between WT and Bid KO. Percent of OT-2 cells found in each division from 3 mice per
group is shown (open bar WT, closed bar Bid KO). Students' T-test P values are depicted as
follows: *, P < 0.05; **, P<0.001; *n.s.,* not significant. CFSE T cells showed no proliferation
or activation in mice receiving HEL-pulsed LCs and represented 0.01% of total lymph node
cells (data not shown). OT-2 T cells expanded from 0.55% to 0.73% of total lymph node
cells in mice receiving OVA-pulsed cDCs from WT versus Bid KO mice, respectively
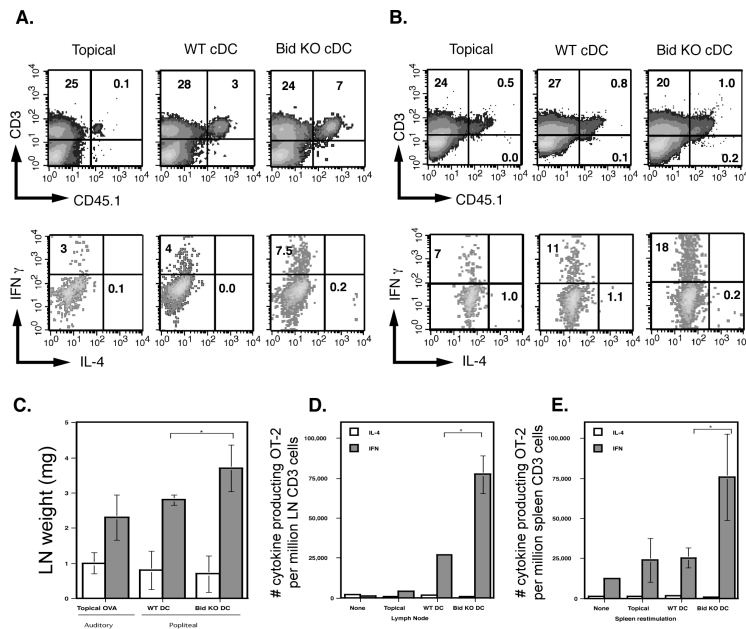(shown in panel A). P<0.05, n=3.

Figure 8. Bid KO cDCs promote increased OT-2 cell expansion and function in lymph node and spleen

cDCs from topically immunized ear skin explants were injected (3×10^5) into the footpad of WT recipient mice (3 per group) containing CD45.1 allotypic OT-2 T cells (2×10^6). Control mice were topically immunized on ears (see Materials & Methods). A. Lymph node cells were harvested after 4 days and stained for CD45.1 to reveal OT-2 T cells (upper panel) that were gated for analysis of cytokine staining (lower panel). B. Spleen cells harvested after 4 days were restimulated with 100 μg/ml OVA in vitro for 3 days prior to CD45.1 and cytokine staining. C. Lymph node weights are increased in mice receiving Bid KO cDCs. Lymph nodes from mice receiving PBS (open bars) or immunization by topical OVA or by cDC transfer (filled bars) were weighed and the mean ± SD per group calculated. *, P < 0.05. D. and E. Bid KO cDCs promote increased numbers of IFNγ producing cells in lymph node (D) and spleen (E). The number of IL-4 (open bar) or IFNγ (filled bar) producing OT-2 cells per million CD3 T cells was calculated for each individual mouse and mean ± SD determined per group. *, P < 0.05. Representative density plots and statistical analyses are shown for one of three independent experiments.

Table I

Lymphoid organ weights and cell yields from WT and Bid KO mice.

Organ [a]	Immunize [b]	Weight (mg)		Cell Yield (x10^6)	
		WT	Bid KO	WT	Bid KO
LN	PBS	6.3 ± 1.2	5.6 ± 0.9	8.4 ± 1.8	9.4 ± 3.8
	OVA	8.8 ± 1.0	10.1 ± 3.8	17.4 ± 5.6	17.3 ± 4.1
$P <$ [c]		n.s. [d]		n.s.	
Spleen	PBS	93.2 ± 4.0	95.4 ± 26.9	72.8 ± 9.9	87.0 ± 21.7
	OVA	93.9 ± 5.9	116.0 ± 7.9	70.3 ± 22.0	87.9 ± 20.9
$P <$		0.05		0.02	

[a] Organs were harvested on day 3 after immunization. LN, Auditory lymph node.

[b] Groups of mice (n=3) were immunized by tape stripping and painted with PBS (control) or 25 μg OVA per ear side. (See Materials and Methods)

[c] P values were determined using a one-tailed, paired Student's t-test comparing OVA immunized WT and Bid KO values. No significant differences were found in PBS treated groups.

[d] n.s., not significant

Table II

Summary of in vitro apoptosis detected in LCs from WT and Bid KO mice.

Exp #[a]	% Specific LC loss[b]		% Specific Apoptosis[c]		% Specific LC Death	
	WT[d]	Bid KO	WT	Bd KO	WT	Bd KO
1	46.7	0.5	21.0	2.0	67.7	2.5
2	47.4	5.0	12.7	3.0	60.1	8.0
3	30.4	7.4	16.0	0.0	46.4	7.4
Average	**41.5**	**4.3**	**16.6**	**1.7**	**58.1**	**6.0**
St Dev	9.6	3.5	4.2	1.5	10.8	3.0
P<[e]		0.02		0.02		0.01

[a] Results from three independent experiments are shown. cDCs were gated for each experiment as follows: Exp # 1, I-A; Exp # 2, CD11c; Exp # 3, Langerin (CD207). WT or Bid KO LCs comprises the majority of cDCs isolated from ear skin cultures, as described in Materials and Methods.

[b] % Specific LC loss is calculated as the difference in percent of LCs remaining after overnight culture in the presence of OVA antigen and relevant OT-2 versus irrelevant 3A9 naïve purified CD4 T cells .

[c] % Specific Apoptosis is calculated as the difference in apoptosis detected by annexin V and/or 7-AAD staining of remaining DCs after overnight culture in the presence of OT-2 or 3A9 T cells.

[d] % Specific LC Death = % Specific LC loss + % Specific Apoptosis.

[e] P values were determined using a one-tailed, paired Student's t-test.